IEEE Transactions on Nuclear Science, Vol.NS-24, No.3, June 1977

EXTRACTION SYSTEM FOR THE CHALK RIVER SUPERCONDUCTING HEAVY-ION CYCLOTRON

C.R. Hoffmann
Atomic Energy of Canada Limited, Chalk River Nuclear Laboratories, Chalk River, Canada K0J 1J0

Summary

The extraction system proposed for the Chalk River heavy-ion superconducting cyclotron is described. The main components are a conventional electrostatic deflector, a pair of passive magnetic lenses and a superconducting magnetic channel. Trim rods are used to generate suitable first harmonic fields to exploit the $\nu_r = 1$ resonance. The lenses are made from saturated iron and are located at the leading and trailing edge of the hill immediately following the dee containing the deflector. The channel has two sections. The first uses saturated iron to give a fixed radial gradient of $\sim$ 30 T/m and superconducting windings to generate a variable bias magnetic field (0.4 T maximum). The second uses superconductors to generate a variable focusing gradient and an independently variable bias field.

Introduction

Single turn extraction from proposed superconducting cyclotrons[1,2] is more difficult than from conventional cyclotrons. High average magnetic fields ($\sim$ 5 T) make electrostatic deflectors less effective and strong radial defocusing gradients along the extraction trajectory make radially compact beams impossible without correspondingly strong compensating elements.

Remedies are available however. Electrostatic deflectors can be located further out in the fringe field where extraction is easier. Magnetically saturated iron, and superconductors serviced from the cyclotron's cryogenic system, can be exploited in focusing elements. Other cyclotron characteristics, particularly high energy gain per turn and a sharp field edge ease extraction as well. These measures are featured in the extraction system to be described.

Figure 1 shows the midplane layout. The broken line through the yoke labelled '0' defines θ=0 for a cylindrical co-ordinate system with its origin at the machine center. The deflector subtends 31° and the beam enters it at θ=162° with radius $\simeq$ 0.65 m. The integral radial resonance produces a turn separation of at least 5 mm at this entrance. Two saturated iron lenses in the following hill inhibit radial beam growth and assist beam deflection because of their intrinsic negative bias fields (discussed later). Each lens subtends 10°. The entrance to the first of two magnetic channel sections is centered on r = 0.696 m at θ=295°. The minimum turn separation here is > 40 mm. Each section has an independently variable bias field which is adequate to guide all ions outwards along nearly coincident trajectories. The two sections have different focusing requirements. The first section passes through the steep fringe region of a hill, whose gradient (-35 T/m) is roughly constant for all ions, while the second passes through a region whose gradient scales with beam rigidity. It is practical to use saturated iron in the first section to get a fixed radial focusing gradient and to compensate nonlinearities in the transition between regions with superconductors. The second section has a variable focusing gradient obtained with superconductors. The two sections subtend 29° and 45° and have a 6° angular gap between them. A dipole magnet (not discussed) steers the beam into the external beam transport system.

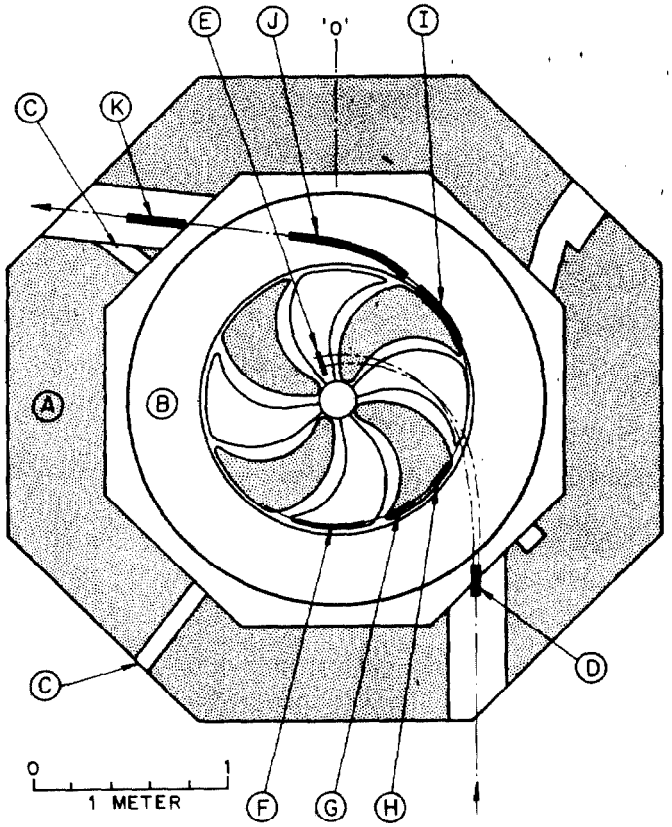

Fig. 1 Midplane plan view of the cyclotron: A - yoke; B - cryostat; C - diagnostic probe holes; D - injection steering dipole; E - stripper foil; F - electrostatic deflector; G,H - hill lenses; I,J - magnetic channel; K - extraction steering dipole.

Resonant Extraction

At the field edge where the radial betatron frequency ν_r is $\sim$ 1 a small first harmonic field of variable amplitude and phase is needed to exploit the integral resonance[3,4]. Such fields can be generated with the outermost set of 60 mm diameter trim rods[5,6]. These rods have their axes at a radius of 0.643 m. They induce symmetric bell-shaped field profiles of $\sim$ 60 mm full width at half maximum amplitude and can easily produce first harmonics of several mT amplitude. Calculations indicate that the amplitude and phase of a 0.5 mT first harmonic can be set to ± 50 μT and ± 6°. For amplitudes required the Walkinshaw resonance causes no significant axial beam growth.

Electrostatic Deflector

Figure 2 shows schematically the cross section of the deflector, which consists of a tungsten septum ($\sim$ 0.5 mm thick), a stainless steel deflector electrode and two tungsten sparking plates. The choice of materials is based on experiments at Michigan State University[7]. The maximum voltage required across the 7 mm aperture is 81 kV. The deflector is located

inside a dee which has the top modified to make space for a high voltage feed line and electrode supports[8].

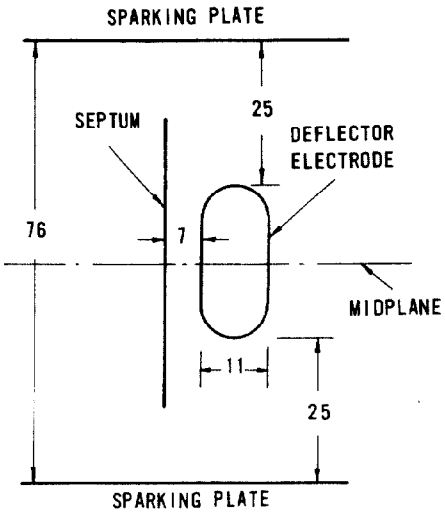

Fig. 2 Cross section of the electrostatic deflector. Units are mm.

Magnetic Elements

Figure 3(a) gives the cross section of the iron bars[9] in the lenses and first channel section. A reference extraction trajectory which is perpendicular to and passes through the cross section at x=0 defines the midplane r-θ shape. Figure 3(b) gives an example of the midplane magnetic field variation, in this case for the first channel section. These geometries produce a significant bias field, that is the field at x=0.

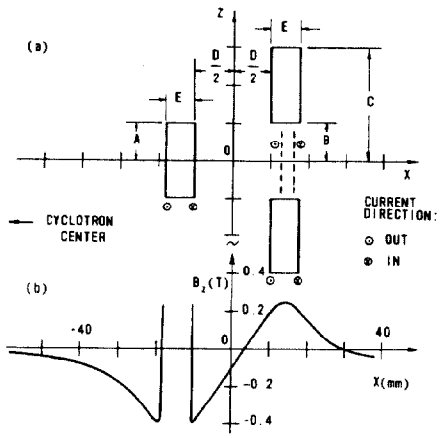

Fig. 3 (a) Cross section of the gradient producing components of the magnetic channel. The heavy vertical lines represent current sheets. The dashed lines are compensation current sheets (see text).

(b) Midplane field B_z from the iron in the first channel section, at the mid-channel cross section.

In general the fields and derivatives are calculated numerically using the Biot-Savart law. The uniform magnetization approximation allows the iron to be modelled as vertical current sheets of surface current density $J_s = 1.72 \times 10^6$ A/m. Analytic solutions exist if the current sheets are considered straight and infinite, which allow quick selection of cross section parameters. For example, the midplane field B_z at any x for such a current sheet in the plane x=L bounded between Z_1 and Z_2 is (MKS units)

$$B_z = 2 \times 10^{-7} J_s \left\{ \tan^{-1}\left(\frac{Z_2}{L-x}\right) - \tan^{-1}\left(\frac{Z_1}{L-x}\right) \right\}.$$

Parameters can be easily found which make dB_z/dr constant to ± 3% over 70% of the aperture.

Figure 3(a) also gives the cross section of the second channel section gradient winding, but the vertical surfaces represent real current flowing in superconductors rather than equivalent surface current of iron. An appropriate superconductor is Nb_3Sn multifilament twisted wire 0.5 mm in diameter with critical current ∿ 300 A in a 5 T field. Two layers give $J_s \sim 1.5 \times 10^6$ A/m, i.e. over 85% the value for saturated iron.

The dashed lines in Fig. 3(a) represent superconductor current sheets to compensate field edge nonlinearities at the first section location, which cause "C"-shaped distortion in radial emittance diagrams. These sheets subtend 29° and dimensions are separation 4 mm and total height 20 mm.

Figure 4(a) shows the cross section of the bias windings for the two channel sections and Fig. 4(b) gives the midplane B_z for the winding current set for -0.3 T. Bias field value and direction required depend on beam rigidity.

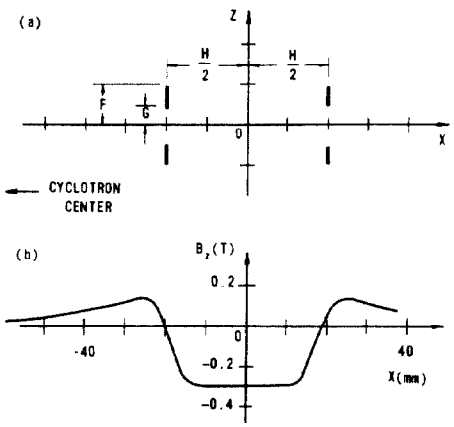

Fig. 4 (a) Cross section of the bias windings.

(b) Midplane field B_z from the bias winding in the first channel section, at the mid-channel cross section.

Table 1 summarizes present choices for the parameters defined in Figs. 3 and 4 and gives values of gradients and bias fields. The bias fields are the sum of the contributions from both the bias and the gradient field structures.

Table 1. Cross section parameters (mm), bias field B_f(T) and gradient dB/dr(T/m) values for the magnetic extraction elements.

	Lenses 1 and 2	Channel Section 1	Channel Section 2
A=B	8	10	12
C	15	30	35
D	16	20	24
E	1.8	8	8
F	-	10	12
G	-	5	6
H	-	37	41
B_f	-0.05	-0.4 to +0.2	-0.2 to +0.12
dB/dr	13.5	30	5 to 18

The channel sections are entirely enclosed within the main cryostat. The inner wall is bulged to fit the first section partially into the hill gap. A helium gas cooled beam pipe separates the beam from channel components. The pipe reduces the aperture D by approximately 6 mm [10].

Calculated Performance

Figure 5 gives calculated radial and axial emittance diagrams at three locations along the extraction trajectory for C^{+6} at 50.5 MeV/u. (Calculations for ions requiring the extreme magnetic fields of 2 and 5 T yield similar results.) This beam requires an average field of 3 T and is the most difficult to deflect. It needs a first harmonic amplitude of 0.75 mT. The calculations use square emittance diagrams 2 mm x 2 mm at the deflector entrance centered on r = 0.653 m. These diagrams nominally enclose the phase space areas the real beam is expected to occupy. At this location ν_r is $\sim$ 0.65, the energy gain per turn is 3.19 MeV, and beam distortion induced from traversing the fringe field to get to the deflector entrance is small. The radial and axial diagrams are horizontal in the steering magnet with total widths of $\sim$ 10 mm.

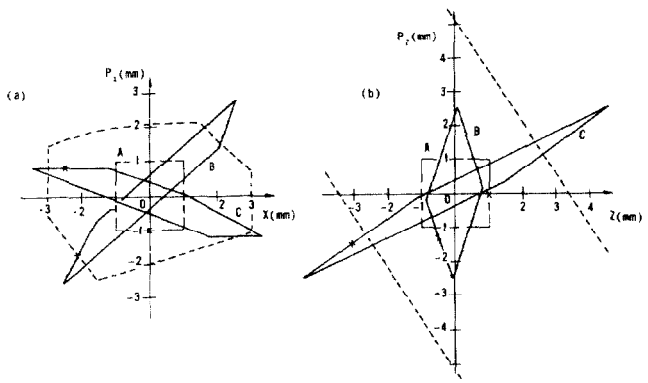

Fig. 5 Plots of radial (a) and axial (b) emittance diagrams and the extraction system acceptance (dashed lines) at the deflector entrance for C^{+6} at 50.5 MeV/u. Momentum is plotted in units (p/qB) x 10^3 mm where p, q and B are momentum, charge and average magnetic induction in MKS units. A - deflector entrance; B - entrance, first channel section; C - exit, second channel section.

The radial and axial acceptances of the system at the deflector entrance are shown dashed in Fig. 5. They have areas about 5 and 25 times those of the emittance squares at the entrance and hence allow 100% efficient beam extraction.

References

1. J.H. Ormrod, C.B. Bigham, J.S. Fraser, E.A. Heighway, C.R. Hoffmann, J.A. Hulbert, P.W. James, H.R. Schneider and Q.A. Walker, "The Chalk River Superconducting Heavy-Ion Cyclotron", Proceedings of this conference.

2. H.G. Blosser, D.A. Johnson and R.J. Burleigh, R.C. Niemann and J.R. Purcell, "Superconducting Cyclotrons", Proceedings of the 7th International Conference on Cyclotrons and their Applications, Zurich, 1975, p. 584.

3. M.M. Gordon, IEEE Trans. Nucl. Sci., NS-13, 48 (1966), "Single Turn Extraction".

4. H.G. Blosser, M.M. Gordon and T.I. Arnette, Nucl. Instr. and Methods 18-19, 488 (1962), "Resonant Extraction from Three-sector Low Spiral Cyclotrons".

5. C.B. Bigham, Nucl. Instr. and Methods 131, 223 (1975), "Magnetic Trim Rods for Superconducting Cyclotrons".

6. E.A. Heighway, "Movable Steel Trim Rods and the Orbit Dynamics of the Chalk River Superconducting Heavy-Ion Cyclotron", Proceedings of this conference.

7. H.G. Blosser, private communication, 1976.

8. C.B. Bigham, "Modelling of the Chalk River Superconducting Heavy-Ion Cyclotron rf Structure", Proceedings of this conference.

9. B. Carbonel, V.I. Danilov, M. Ianovici and E.A. Polferov, Nucl. Instr. and Methods 84, 144 (1970), "Calculation of the Geometry of Magnetic Channels for Synchrocyclotrons and Cyclotrons".

10. J.A. Hulbert, private communication, 1976.